Check for updates

Long-term performance of a hybrid indirect evaporative cooling-mechanical vapor compression cycle: A case study in Saudi Arabia

Qian Chen[1]*, Kum Ja M[1], Muhammad Burhan[1], Muhammad Wakil Shahzad[2], Doskhan Ybyraiymkul[1], Seungjin Oh[3], Xin Cui[4] and Kim Choon Ng[1]*

[1]Water Desalination and Reuse Center, Biological and Environmental Science and Engineering Division, King Abdullah University of Science and Technology, Thuwal, Saudi Arabia, [2]Department of Mechanical and Construction Engineering, Northumbria University, Newcastle Upon Tyne, United Kingdom, [3]Clean Innovation Technology Group (Jeju Regional Division), Korea Institute of Industrial Technology (KITECH), Jeju, South Korea, [4]Institute of Building Environment and Sustainable Technology, Xi'an Jiaotong University, Xi'an, China

In Saudi Arabia, air conditioning is the main consumer of electricity, and increasing its energy efficiency is of great importance for energy conservation and carbon footprint reduction. This study presents the evaluation of a hybrid indirect evaporative cooling-mechanical vapor compression (IEC-MVC) cycle for cooling applications in Saudi Arabia. Most cities in this country are characterized by a high sensible cooling demand, and a few cities near the coasts of the Red sea and the Persian Gulf also need dehumidification. By employing the hybrid system, IEC can undertake about 60% of the cooling load in the summer of arid cities, and energy consumption can be reduced by up to 50%. The contribution of IEC and energy saving are less significant in humid cities because the latent loads have to be handled by MVC. Over the whole year, IEC contributes 50% of the total cooling capacity and reduces energy consumption by 40% in dry cities, while the saving is lower at 15%−25% in humid cities like Mecca and Jeddah. The average water consumption of the IEC is in the range of 4−12 L/hr. The water consumption can be replenished by the condensate collected from the MVC evaporator if the ambient humidity is high. Based on the annual performance, the cost of the IEC-MVC process is calculated, and it is 15%−35% lower than the standalone MVC. The results demonstrate the great potential of the hybrid IEC-MVC cycle in Saudi Arabia.

KEYWORDS

indirect evaporative cooling, mechanical vapor compression, long-term analysis, energy saving, water consumption, economic analysis

1 Introduction

Buildings represent a major consumer of electricity in the Gulf Cooperation Council (GCC) region. For example, in Saudi Arabia, all building sectors, including residential, commercial, governmental, and industrial sectors, consume almost 80% of electricity (Krarti et al., 2017). A significant portion of the electricity consumption is attributed to air conditioning, which can account for 50% of the peak electricity demand (Eveloy and Ayou, 2019). Therefore, increasing the energy efficiency of air conditioning systems is crucial for conserving energy and reducing the corresponding CO_2 emission from power plants.

The air conditioning systems in Saudi Arabia are dominated by mechanical vapor compression (MVC) technology. Considering the residential houses alone, more than 24 million MVC units (mainly window units and split units) are installed (Housing GAStat, 2018a). The advantages of MVC include high technology maturity and low initial costs. However, the energy efficiency of MVC is low in Saudi Arabia. This is because the ambient temperature is high, leading to a high condensation temperature. Moreover, the air quality in Saudi Arabia is poor, and corrosion of outdoor condensers is very common (Shahzad et al., 2019; Shahzad et al., 2021). The corroded condensers have extra thermal barriers and further increase the condensation temperature.

The indirect evaporative cooler (IEC) is deemed a promising alternative to MVC and has gained substantial research interest in recent years. It utilizes the evaporation of water to create a cooling effect, and the power consumption is very low. Compared to MVC, the energy efficiency of IEC is several times higher (Jradi and Riffat, 2014). Extensive research efforts have been reported to improve the performance of IEC, including parameter optimization by mathematical modelling (Anisimov et al., 2014; Cui et al., 2014; Heidarinejad and Moshari, 2015; Cui et al., 2016; Zhu et al., 2017; Dizaji et al., 2020), proposing novel configurations (Riffat and Zhu, 2004; Duan et al., 2012; Wang et al., 2017; Boukhanouf et al., 2018; Jia et al., 2019; Pandelidis et al., 2020), adding internal structures to enhance heat and mass transfer (Kabeel and Abdelgaied, 2016; Kabeel et al., 2017; Moshari and Heidarinejad, 2017; Park et al., 2019; Ali et al., 2021), and exploring different materials (Zhao et al., 2008; Lee and Lee, 2013; Boukhanouf et al., 2017; Wang et al., 2017; Rashidi et al., 2019).

As Saudi Arabia is characterized by high ambient temperatures, IEC is highly applicable and has huge potential for energy saving. However, IEC is a passive cooler and the outlet temperature is highly dependent on the inlet temperature. When the outdoor temperature is extremely high, the supply air from IEC cannot achieve room thermal comfort. Another limitation of IEC is the lack of dehumidification capability, which restricts its application to dry areas (Chen et al., 2022).

To address the limitations of IEC, several researchers have proposed the hybridization of IEC with MVC. In the hybrid cycle, IEC is used to pre-cool the outdoor air, and then MVC further reduces the temperature and humidity (Chen et al., 2021). Such a hybrid process combines the advantages of the two, i.e. IEC's high efficiency in sensible cooling and MVC's capability of temperature and humidity control. Its energy-saving potential has been evaluated in several areas, including China (Beijing (Duan et al., 2019) and Xi'an (Cui et al., 2019a)), Iran (Delfani et al., 2010), Italy (Zanchini and Naldi, 2019), and Singapore (Vargas Bautista, 2014; Cui et al., 2015). The energy consumption was observed to be reduced by up to 35% (Cui et al., 2019a).

This study evaluates the potential of the hybrid IEC-MVC cycle in Saudi Arabia. The climatic and geographical conditions of the country are firstly analyzed. Then the daily performance of IEC-MVC on typical days in several cities is investigated on an hourly basis. Afterward, such efforts are extended to the major cities over the whole year to get the annual energy saving, IEC contribution, and water consumption. Finally, the annual cost of IEC-MVC is compared with standalone MVC to demonstrate the economic benefits.

# 2 Regional characteristics of Saudi Arabia

Saudi Arabia is the largest country in the MENA region. It has an estimated land area of 2.15 million square km, spanning 1700 km from north to south and 2000 km from east to west (Mikayilov et al., 2020). The country is divided into 13 provinces, as shown in Figure 1A. Based on the topography and climatic conditions, these provinces are divided into four regions by the Saudi Electricity Company (SEC), namely, the Western region, Eastern region, Central region, and Southern region (Saudi Electricity Company, 2015).

The Central region spans 19–29° north and includes three provinces: Al-Riyadh, Hail, and Al-Qaseem. In the past few decades, it has experienced fast urbanization and economic growth. Currently, it has 32% of the country's population (SAMA, 2019) and the third highest region GDP (GDP per capita = $21,591 (Lopez-Ruiz et al., 2018)). Figure 2 shows the total floor areas of living houses in each province. Most houses in the central region are located in the Al-Riyadh province, which holds the capital city Riyadh. More than half of the houses are villas, while the share of apartments and traditional houses is small.

The Eastern region covers 19–32° north and consists of three provinces: Eastern Region, Al-Jouf, and Northern Borders. It has the largest land area and second population density (2018 people per km² (SAMA, 2019)). The East region is famous for its industrial activities, as it contains the country's most immense oil reserves. Most of the houses in the Eastern region are villas and apartments, and they are
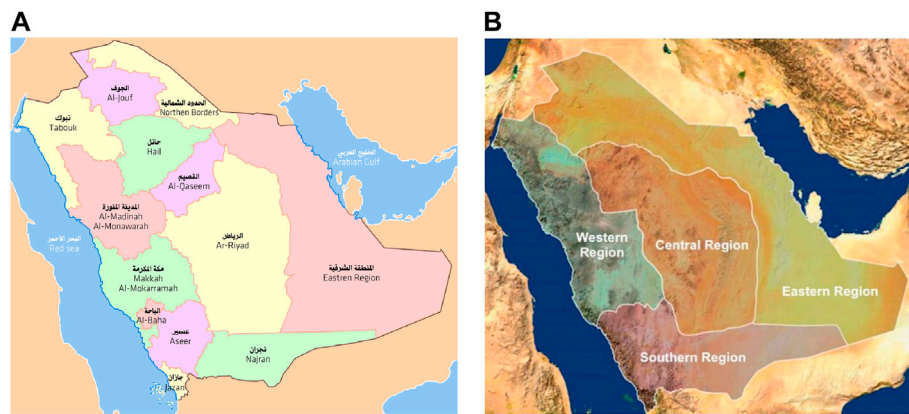
FIGURE 1
(A) Provinces (Provinces of Saudi Arabia, 2015) and **(B)** operating regions (Saudi Electricity Company, 2015) of Saudi Arabia.
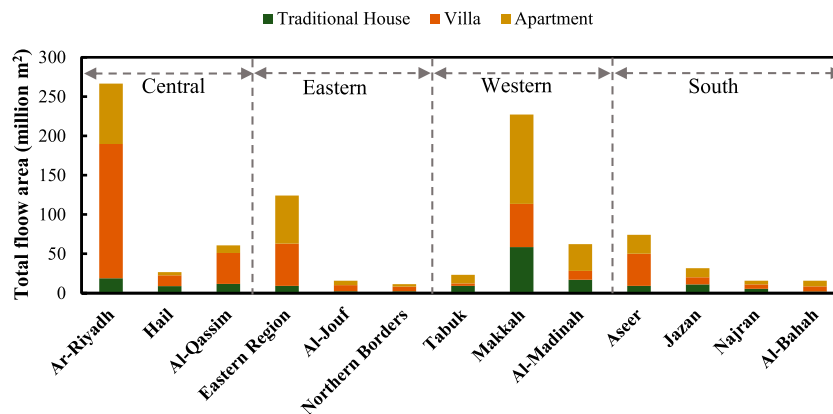
FIGURE 2
Total floor area per housing type in different provinces of Saudi Arabia.

mainly located near the Persian Gulf in the Eastern region province.

The Western region is located on the coast of the Red Sea (19–30°north), and it consists of three provinces: Tabouk, Makkah, and Al-Madinah. This region is home to many important cities, including Jeddah, Mecca, and Medina. The former is the commercial center of Saudi Arabia, and the latter two are the holiest sites for Muslims. The Western region houses 35% of the country's population and the population density is the highest (3423 people per km²) (SAMA, 2019). The total floor area in the Western region is as large as that of the Middle region, but nearly half of them are apartments. As apartments are better conditioned (52% of the livable floor area is cooled, as compared to 45% for villas

(Housing GAStat, 2018b)), a higher share of apartments will lead to higher cooling energy consumption.

The South region spans 16–21° north and consists of Aseer, Jazan, Najran, and Al-Bahah. It has fertile land and adequate water reserves and is a place for agriculture and tourism. It houses only 15% of the country's population and the population density is 1871 people per km² (SAMA, 2019). The total house area is only 138 million m², much smaller than other provinces.

Due to its vast territory, Saudi Arabia has a variety of climatic conditions. Figure 3A shows the annual climatic data of Riyadh, the most important city in the Central region. The weather is hot and dry in the summer, as it is in the desert area and has no access to any natural water source. The maximum temperature exceeds 40 °C in the summer, while the RH is below 15%. The winter
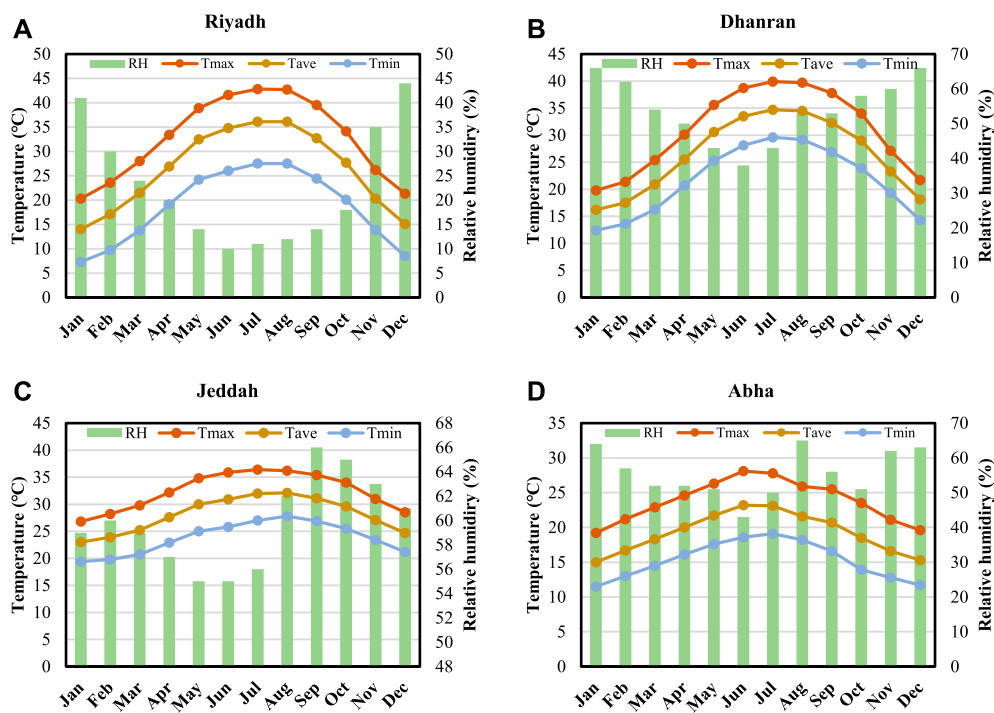
FIGURE 3
Annual weather data for representative cities of four regions: **(A)** Central region-Riyadh, **(B)** Eastern region-Dhanran, **(C)**, Western region-Jeddah and **(D)** Southern region-Abha (Wunderground, 2022).

months, on the other hand, have a low ambient temperature due to the high altitude (~600 m). Therefore, in addition to cooling, there is also a need for heating.

Figure 3B shows the weather condition of Dharan, one of the biggest cities in the Eastern region. The ambient temperature varies in a similar way to that of Riyadh, i.e. hot in summer and cold in winter. However, the humidity in Dharan is higher (RH = 40%–65%), as it is close to the Persian Gulf. Therefore, it needs both cooling and dehumidification in the summer.

The Western region receives hot and humid air from the Red sea, and most cities in this region have high humidity and temperature. Figure 3C shows the monthly weather data of Jeddah, the largest city in the Western region. The ambient temperature is 20–35°C throughout the year, and the RH is always higher than 50%. The high temperature and humidity from the outdoor ambient will add substantial sensible and latent cooling loads to the buildings.

Most areas in the South region have a high altitude of >1000 m, making the ambient temperature lower than in other regions. As can be seen in Figure 3D, the ambient temperature in summer is lower than 30°C, and the need for cooling is minimum. The ambient humidity is also low, and there is little need for dehumidification.

The annual need for cooling is usually quantified by cooling degree-days (CDD). CDD is calculated by adding up the

difference between the daily-average temperature and a standard temperature (usually 18°C). One limitation of CDD is that it is calculated on a daily basis and does not account for the dynamical variation of the ambient condition. Even if the CDD is 0, there is still a need for cooling at the noon time. To overcome such a limitation, we propose to calculate the cooling needs based on the hourly data, i.e. cooling degree-hours (CDH) (Chen et al., 2022).

$$CDH = \sum \left(T_{hourly} - 18°C \right) when\, T_{hourly} > 18°C \qquad (1)$$

Both CDD and CDH consider only the sensible cooling load and neglects the latent load. To assess the latent load, we introduce the dehumidifying gram hours (DGH), which quantifies the amount of moisture that needs to be removed from the ambient air (Chen et al., 2022)

$$DGH = \sum \left(\omega_{hourly} - 9\, \frac{g}{kg} \right) when\, \omega_{hourly} > 9\, \frac{g}{kg} \qquad (2)$$

where ω_{hourly} is the humidity ratio of the ambient air.

Figure 4 summarizes the CDH and DGH for representative cities in different provinces of Saudi Arabia. It is obvious that the CDH values are very high in most cities. For example, the CDH for Riyadh is 92,248.4°C-hr/year. If averaged over the whole year (8760 h), the outdoor temperature has to be cooled
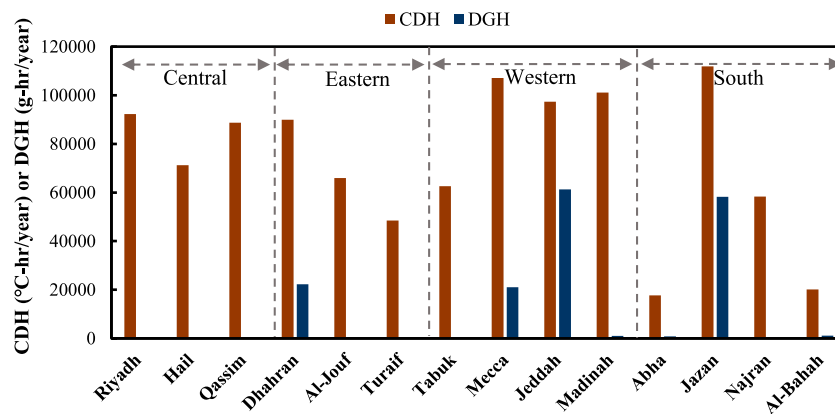
FIGURE 4
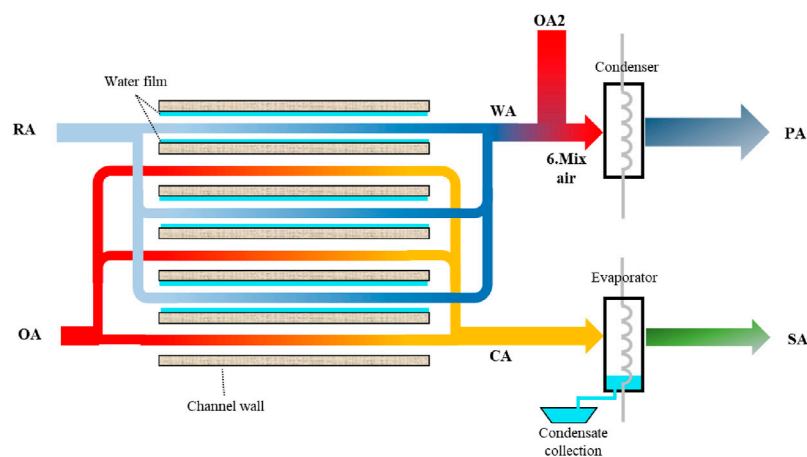CDH and DGH for representative cities of Saudi Arabia.

FIGURE 5
Annual weather data for representative cities of four regions.

by 10.4°C before being supplied to the room. Qassim, Dhahran, Mecca, Jeddah, Madinah, and Jazan also have CDH that are close to or higher than 9000°C-hr/year. The exception occurs in the Southern region, i.e. Abha (CDH = 175647.9°C-hr/year) and Al-Bahah (CDH = 20167.7°C-hr/year).

The DGH in most cities are below 1000 g-hr/year, indicating little need for dehumidification. However, there are several cities that are close to the sea (Red sea or Persian Gulf), and their DGH values are very high. These cities include Dhahran (DGH = 22,225 g-hr/kg), Jeddah (DGH = 61,307 g-hr/kg), Mecca (DGH = 22,225 g-hr/kg) and Jazan (DGH = 58,262 g-hr/kg).

3 Hybrid IEC-MVC

To improve the energy efficiency for cooling, we have proposed a novel cooling cycle combining indirect evaporative cooling (IEC) and mechanical vapor compression (MVC) (Chen et al., 2021; Chen et al., 2022). Figure 5 depicts the schematic of the hybrid IEC-MVC cycle. The IEC consists of alternating dry and wet channels. The outdoor air (OA), which is hot and sometimes humid, is supplied to the dry channels of the IEC, and the room return air (RA) passes through the wet channels. Simultaneously, water is sprayed into the wet channels from their entrances. As RA is unsaturated, the sprayed water evaporates and absorbs heat from the wet channels, which further cools OA

TABLE 1 Correlations for evaluating the IEC-MVC cycle.

Equation	No.	Comments
$\varepsilon_{IEC} = \min\left\{\dfrac{h_{OA}-h_{CA}}{h_{OA}-h_{sat}(T_{RA})}, \dfrac{h_{WA}-h_{RA}}{h_{sat}(T_{OA})-h_{RA}}\right\}$	(3)	The effectiveness of IEC calculated from the inlet and outlet air conditions, including temperature, humidity and flowrate (Chen et al., 2021)
$\omega_{IEC} = \min\left\{\omega_{OA}, \omega_s(h_{CA})_{|RH=100\%}\right\}$	(4)	Air humidity leaving IEC
$T_{IEC} = T(h_{CA}, \omega_{IEC})$	(5)	Air temperature leaving IEC
$P_{IEC} = P_{pump} + P_{fan,IEC}$	(6)	Power consumption of IEC
$COP_{IEC} = \dfrac{\dot{m}_{OA}(h_{OA}-h_{CA})}{P_{IEC}}$	(7)	Energy efficiency of IEC
$P_{MVC} = P_{comp} + P_{fan,MVC}$	(8)	Power consumption of MVC
$COP_{MVC}\dfrac{\dot{m}_{OA}(h_{OA}-h_{SA})}{P_{MVC,standalone}}$	(9)	Energy efficiency of MVC
$COP_{IEC-MVC} = \dfrac{\dot{m}_{OA}(h_{CA}-h_{SA})}{P_{IEC}+P_{MVC,hybrid}}$	(10)	Energy efficiency of hybrid IEC-MVC
$\varnothing_{IEC} = \dfrac{h_{OA}-h_{CA}}{h_{OA}-h_{SA}} \times 100\%$	(11)	Contribution of IEC to overall cooling load
$\Delta P = \dfrac{COP_{IEC-MVC}-COP_{MVC}}{COP_{IEC-MVC}}$	(12)	Energy-saving of IEC-MVC over MVC
$\dot{m}_{consumption} = \dot{m}_{RA}(\omega_{WA}-\omega_{RA})$	(13)	Water consumption in IEC wet channels
$\dot{m}_{collection} = \dot{m}_{OA}(\omega_{CA}-\omega_{SA})$	(14)	Condensation collection from MVC evaporator
$\dot{m}_{water} = \dot{m}_{consumption} - \dot{m}_{collection}$	(15)	Net water consumption

FIGURE 6
Computational algorithm for evaluating the hybrid IEC-MVC cycle.

in the dry channels. The pre-cooled outdoor air (CA) then passes the evaporator of a conventional MVC cycle to be further processed to the desired condition before entering the room. The moisture contents formed in the evaporator are collected and reused as part of the water source for the wet channels. The air leaving the wet channels of IEC (WA) is also reused in the MVC: it is mixed with the outdoor air to function as the heat sink of the condenser.

A pilot IEC-MVC unit has been constructed and tested in our previous study (Chen et al., 2021; Chen et al., 2022). The tests cover a wide range of ambient conditions (temperature 30–45°C, humidity ratio 10–20 g/kg). Based on the test data, the performance of the system is correlated to the climatic data (temperature and humidity) and the operating conditions (air flowrate and desired supply air conditions), as summarized in Table 1. The model demonstrated high agreement with the experimental data, and the discrepancies are within 4%. The developed correlations can be used to predict the long-term performance of IEC-MVC.

Employing the developed correlations, the annual energy-saving potential of the hybrid IEC-MVC process is assessed. When the outdoor air temperature is below 26°C, IEC is bypassed as it has little energy-saving (Chen et al., 2021; Chen et al., 2022), and only MVC is operated. Otherwise, the outdoor air is pre-cooled in IEC before going to MVC. The outdoor air is finally processed to 18°C and <9 g/kg to sustain indoor thermal comfort (ANSI/ASHRAE Standard 55-2020, 2020). If the absolute humidity is below 9 g/kg, cooling the air to 18°C is sufficient. However, when the humidity is higher than that, outdoor air is cooled down to 12°C so that the moisture content can be reduced to 9 g/kg. The computational algorithm is depicted in Figure 6. Thermodynamic properties of the air are calculated based on the temperature and humidity using the equations developed by Herrmann, Kretzschmar, and Gatley (Herrmann et al., 2009).

4 Performance analysis

Employing the developed model, we evaluate the annual performance of the hybrid IEC-MVC system under the weather conditions of 14 cities in Saudi Arabia. Standalone MVC is also evaluated under the same conditions as a reference system. The analysis is performed on an hourly basis to get the energy efficiency, net water consumption, and IEC contribution. Without loss of generality, the outdoor air flowrate is assumed 1 kg/s, and the results can be extended to any air flowrate.

Figures 7A,B show the variation of air temperatures and humidity on a typical summer day (27 July 2021) in Riyadh. As described previously, Riyadh is hot and dry in the summer. The ambient temperature is 35–45°C, while the humidity ratio is below 7 g/kg. Therefore, the hybrid cooling process only needs to
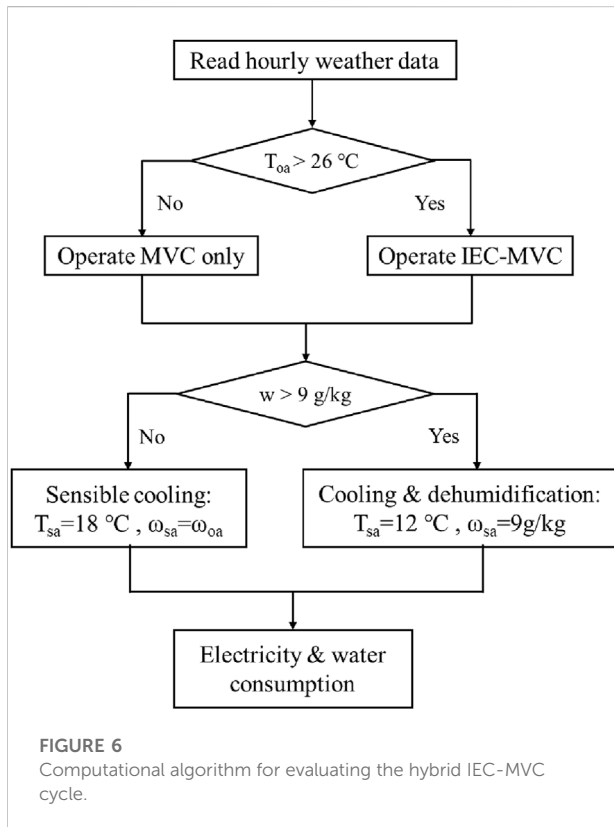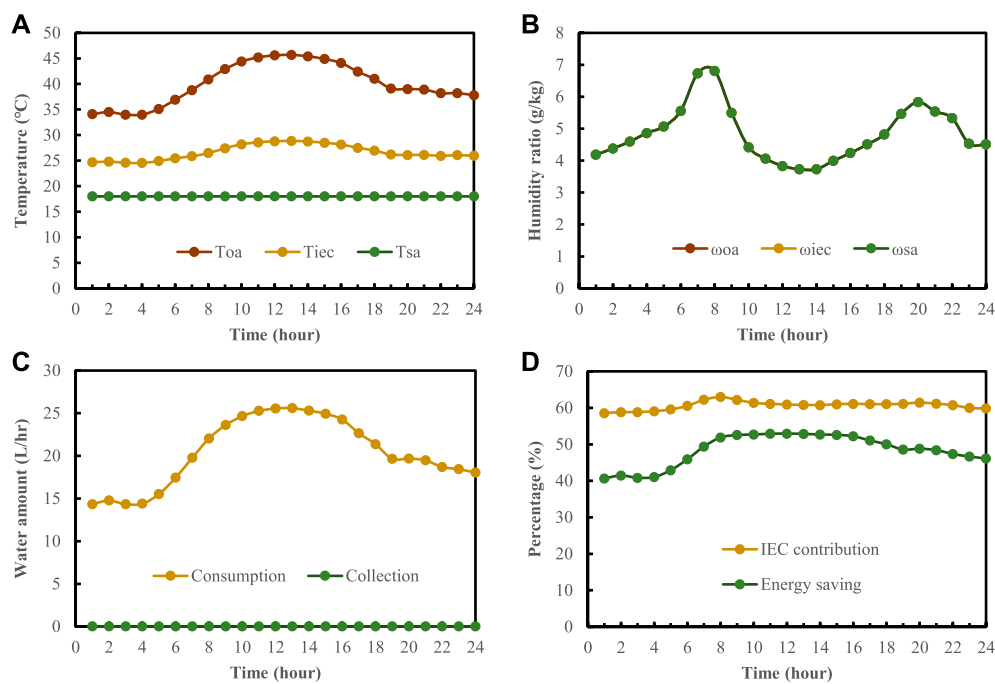
FIGURE 7
Daily performance of IEC-MVC in Riyadh on Jul-27 2021: **(A)** temperature change, **(B)** humidity change, **(C)** water collection and consumption, and **(D)** $\varnothing_{IEC}$ and energy saving.

reduce the air temperature, while the absolute humidity of the air remains the same. As IEC is a passive cooler (Chen et al., 2020; Chen et al., 2021), the air temperature leaving IEC follows the same trend as the outdoor air. The air temperature can be reduced by 9–17°C in IEC, and more temperature drop is observed during 10:00–16:00 when the ambient is hot. After pre-cooling in IEC, the air temperature is 24–29°C and is further cooled to 18°C by MVC.

Figure 7C shows the amount of water consumed by the IEC. Depending on the ambient temperature, the water consumption varies during the day and is in the range of 15–25 L/h. More water is consumed at noontime due to a higher cooling load. On the other hand, there is no water collection from the evaporator, as the outdoor air is dry. The contribution of IEC to the total cooling capacity is about 60% throughout the day, as plotted in Figure 7D. The corresponding energy saving over standalone MVC is 40%–53%, and more saving is observed at noontime. Similar observations were also reported by other studies (e.g., Cui et al. (Cui et al., 2019a)), as IEC has higher COP when the outdoor temperature is higher (Chen et al., 2020; Chen et al., 2021).

Figure 8 summarizes the performance of the system in Dharan, a hot and humid city in the Eastern region. The ambient temperature is similar to that of Riyadh, while the humidity is much higher. The absolute humidity during the daytime is 10–16 g/kg and exceeds 20 g/kg at night. Because

of the higher humidity, IEC demonstrates a different performance from the case of Riyadh, and the outlet air temperature of IEC does not follow the ambient anymore. As shown in Figure 8A, the IEC outlet temperature increases during 17:00–23:00, although the ambient temperature shows a descending trend. This is because the air temperature is lower than its dew point temperature, and condensation occurs. This can be clearly seen in Figure 8B, which shows a drop in air humidity along IEC during this period. The released condensation heat increases the air temperature. The MVC further cools down the air to a low temperature of 12°C, as opposed to 18°C in the previous case. This is to dehumidify the air to 9 g/kg.

The water consumption of IEC is in the range of 10–28 L/h, and the peak is observed at noon, as shown in Figure 8C. Such amount of water consumption can be replenished by the condensate collected from the MVC evaporator. The daily-average water consumption is 18.7 L/h, while condensate generation is 25.7 L/h due to very high humidity at night. The excessive water can be used elsewhere in the house. Figure 8D plots the contribution of IEC and the corresponding energy saving. IEC undertakes 20%–45% cooling load, much lower than the case of Riyadh. This is attributed to a latent load that is mostly handled by MVC. Due to a smaller IEC contribution, the energy saving is also less at 10%–35%.
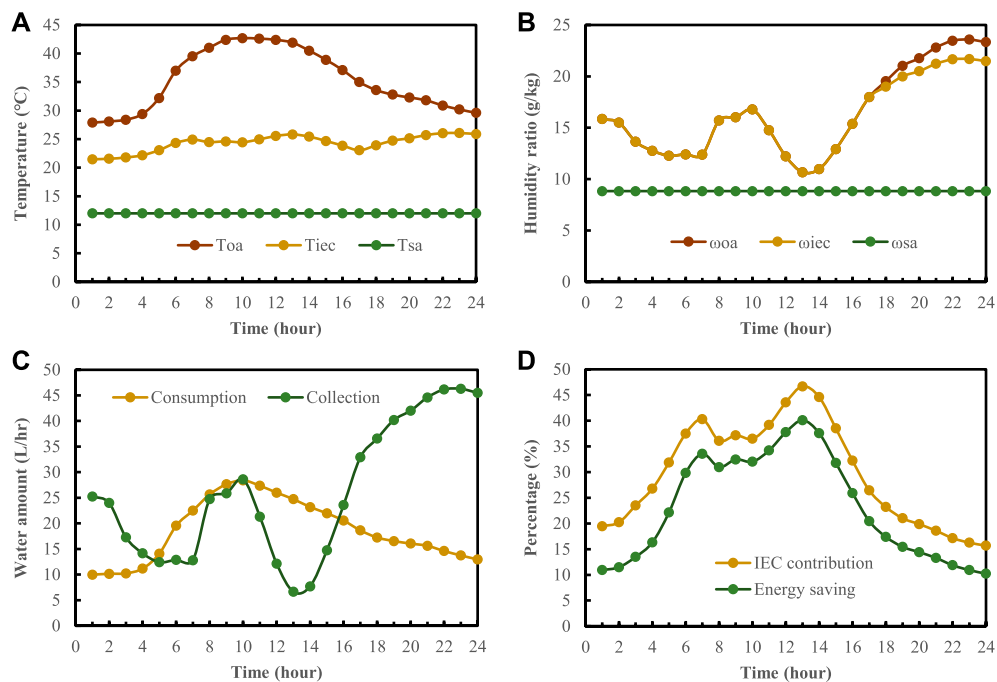
FIGURE 8
Daily performance of IEC-MVC in Dharan on Jul-15 2021: **(A)** temperature change, **(B)** humidity change, **(C)** water collection and consumption, and **(D)** $\varnothing_{IEC}$ and energy saving.

Figure 9 plots the system performance on a summer day (15 July 2021) in Jeddah. The weather condition differs from Riyadh and Dharan. Firstly, the ambient temperature is slightly lower, and the peak temperature is below 40℃. Secondly, the humidity ratio is high at 17–18 g/kg throughout the day. Due to these unique features, the outlet air temperature from IEC is relatively stable, as plotted in Figure 9A. This is because the low ambient temperature is compensated by the condensation heat released from the wet channels, which can be seen in Figure 9B. Another interesting observation is that the amount of water collection is always higher than water consumption (35.9 L/h vs. 15.5 L/h, shown in Figure 9D), and the amount of excessive water collection is significant. The contribution of IEC to the overall cooling load is lowered to 17%–30%, and the corresponding energy saving is 10%–25%.

The above analyses represent three situations for the application of IEC-MVC: 1) hot and dry weather, where IEC can handle a high portion of cooling load and the energy saving is significant, 2) hot with moderate humidity in the daytime but highly humid at night, where condensate can be collected at night to operate IEC in the daytime, and 3) high air humidity throughout the day, where there is excessive water collection for other uses.
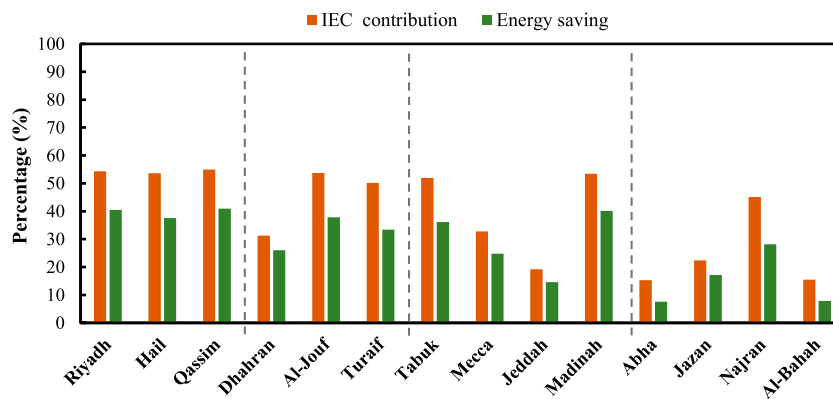
Figure 10 summarizes the energy-saving potential of the hybrid IEC-MVC system over standalone MVC in different cities. The results are based on hour-by-hour simulations using long-term climatic data in each city. As most cities are hot and dry, IEC can meet more than 50% of the annual cooling demand and reduce energy consumption by 40%. The values are very close to the findings reported by Delfani et al. (Delfani et al., 2010), who evaluated IEC-MVC under weather conditions in Iran. For humid cities like Dhahran, Mecca, Jeddah, and Jazan, the latent load is higher and MVC has to contribute more. In this case, the contribution of IEC is smaller at 20%–30%, and the energy saving is less pronounced. Abha and Al-Bahah represent another case that has little cooling demand and little energy-saving potential.

As discussed above, a key challenge in humid areas is the need to overcool the air to remove moisture, and the contribution of IEC is small. To understand the effect of overcooling, the supply air temperature is changed between 11 and 15℃, and the system response is shown in Figure 11. For every ℃ increment of the supply air temperature, the contribution of IEC and the energy saving can be increased by 1%–2%. This is because a higher supply air temperature increases the evaporator temperature and reduces the thermal lift of the MVC compressor (Cui et al., 2019b).
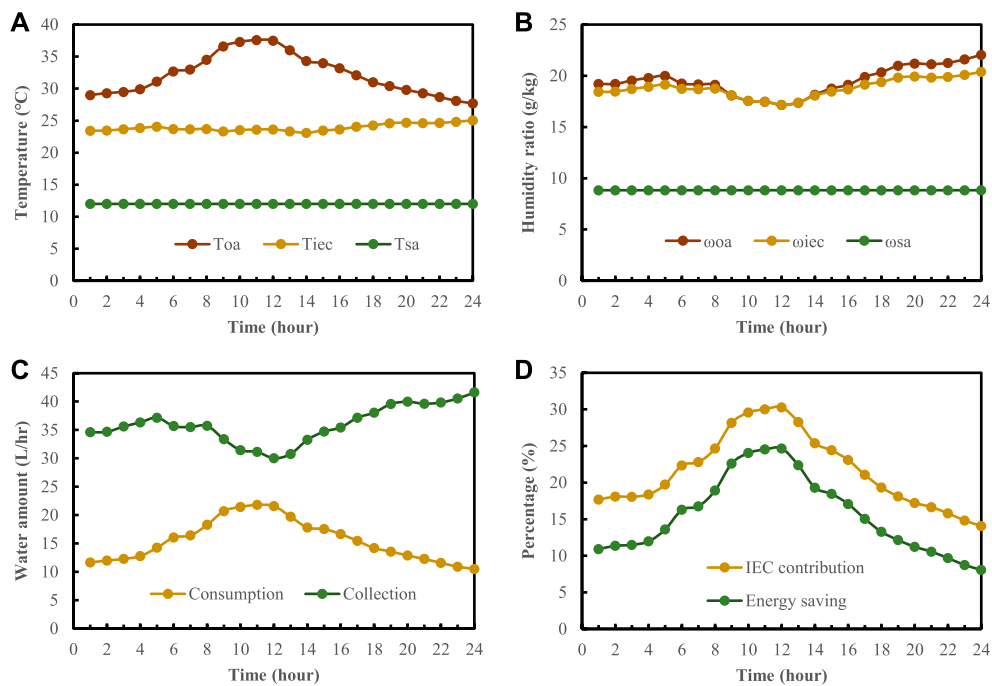
FIGURE 9
Daily performance of IEC-MVC in Jeddah on Jul-15 2021: **(A)** temperature change, **(B)** humidity change, **(C)** water collection and consumption, and **(D)** $\varnothing_{IEC}$ and energy saving.
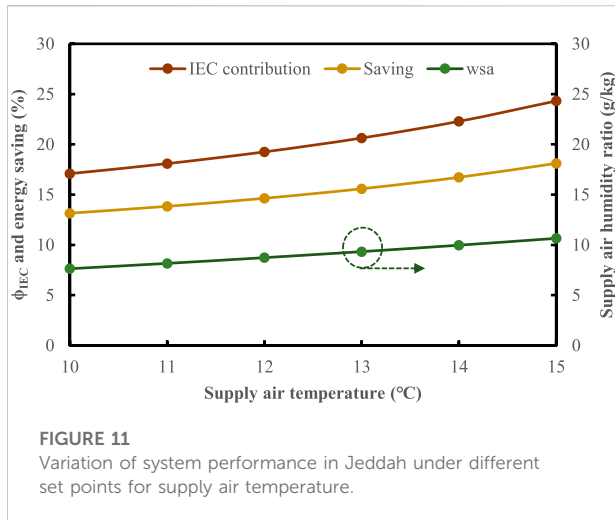

FIGURE 10
Annual energy saving and contribution of IEC in different cities.

Although the humidity ratio is also higher, the value is still below 10 g/kg until 14°C.

Figure 12 summarizes the annual water consumption of IEC and the amount of condensate collected from the MVC evaporator. For cities with certain cooling demands, the annual average water consumption is 4–12 L/h, depending on

the cooling load of IEC. More water is consumed in cities like Mecca, Jeddah, Madinah, and Jazan, where the CDH is very high, as previously shown in Figure 4. On the other hand, there is little water collection in most of the cities because of the dry ambient, and the water consumption for IEC has to be supplied by an external source. The exceptions are Dhahran, Mecca, Jeddah, and

FIGURE 11
Variation of system performance in Jeddah under different set points for supply air temperature.

TABLE 2 Economic parameters for IEV-MVC and standalone IEC.

Parameter	Value	Source
System lifespan (years)	20	Vargas Bautista, (2014)
Interest rate	2%	Saudi Arabia interest rate, (2022)
MVC initial cost ($/Rton)	500	From manufacturer quotation
IEC initial cost ($/CMH)	0.5	From manufacturer quotation
Electricity price ($/kWh)	0.048	Electricity price in Saudi Arabia, (2022)
Water price ($/m³)	0.038	Saudi Arabia water price, (2022)

Jazan. In Dharan and Mecca, the collected condensate can compensate for most of the water consumption. In the cases of Jeddah and Jazan, the amount of condensate is much higher than the water consumption, and there is excessive water to be used elsewhere.

5 Economic analysis

Based on the long-term performance, we evaluate the economic benefits of using the hybrid IEC-MVC process. Similar to the previous section, the evaluation is based on an outdoor flowrate of 1 kg/s. The annual cost is calculated as

$$C_{annual} = C_0 \times CRF + P_{elec} \times c_{elec} + m_{water} \times c_{water} \qquad (16)$$

where C_0 is the initial cost, CRF is the capital recovery factor, P_{elec} and m_{water} are the annual electricity and water consumption, respectively, and c_{elec} are c_{water} the prices of water and electricity, respectively.

The capital recovery factor is calculated from the annual interest rate (i) and the lifespan (n)

$$CRF = \frac{i \times (1 + i)^n}{(1 + i)^n - 1} \qquad (17)$$

Both systems are assumed to have a lifespan of 20 years, and the annual interest rate is 2%. The system capacities are determined by the peak load, which can be extracted from the calculations shown in the previous section. Water and electricity prices are $0.048/kWh and $0.04/m³, respectively. The economic parameters are summarized in Table 2.

Figure 13 summarizes the annual costs of both systems in different cities. It can be clearly seen that the costs are higher in Dhahran, Mecca, Jeddah, and Jazan, as they have very high demands for sensible cooling and dehumidification, leading to high system capacity. Other cities need only sensible cooling and the design loads are much lower. Compared
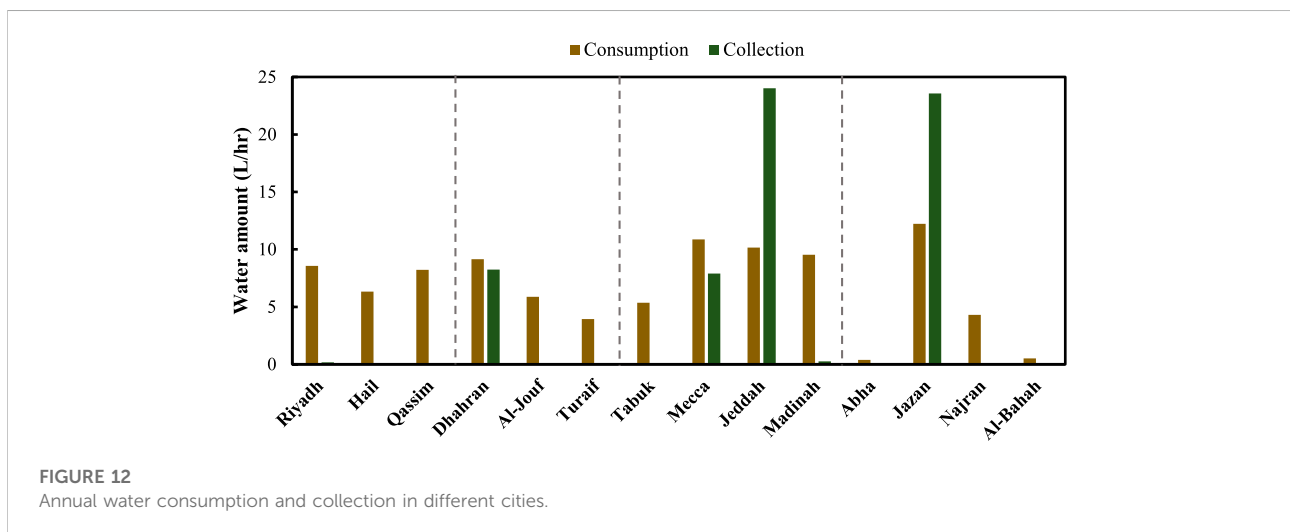
FIGURE 12
Annual water consumption and collection in different cities.
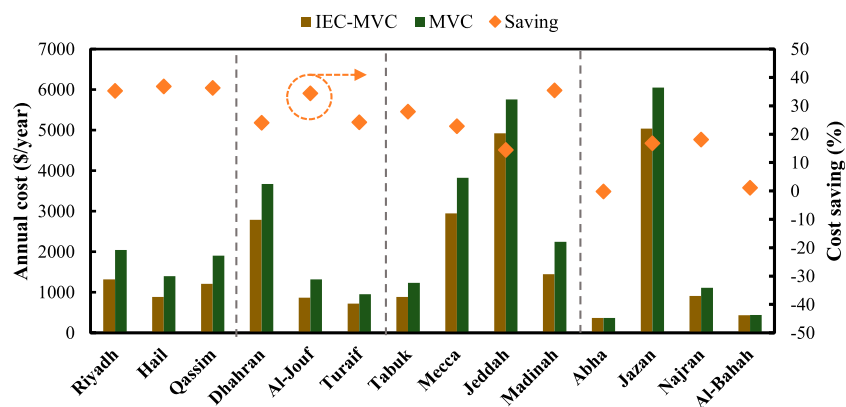
FIGURE 13
Comparison of annual cost between IEC-MVC and standalone MVC.

with standalone MVC, the hybrid IEC-MVC can reduce the annual cost by 15–35%. The cost saving is more significant in dry cities like Riyadh, Hail, Qassim, and Al-Jouf. This is because more cooling load is handled by IEC, which has lower initial costs and energy consumption.

6 Conclusion

This study evaluates the long-term performance of the hybrid IEC-MVC cycle in Saudi Arabia. The climatic and geographical conditions of different cities are firstly analyzed, followed by the daily performance profile of the system under representative cities. Afterward, the annual energy-saving potential of the hybrid system in different cities is summarized, and the economic benefits are quantified. The main takeaways from the study include:

1) Most of the residential houses are located in three provinces, i.e. Al-Riyadh, Eastern region, and Makkah. Al-Riyadh is characterized by hot and dry ambient in the summer, with annual CDH and DGH of 92248.4°C-hr/year and 0 g-hr/year, respectively. The other two provinces are hot and humid, and with DGH >20,000 g-hr/year;

2) In the summer days of Riyadh, the IEC can contribute nearly 60% of the total cooling load, reducing energy consumption by up to 50%. The savings are less significant in Dharan and Jeddah due to a high humidity ratio, as MVC has to cool the air to a lower temperature to remove the moisture;

3) Over the whole year, IEC can handle >50% of cooling load in arid cities and the energy consumption is lowered by 40%. In humid cities, the contribution of IEC is reduced to 40%, and the energy saving over standalone MVC is 15–25%;

4) The energy consumption in humid cities can be further reduced by increasing the supply air temperature, and

every °C increment of the supply air temperature will lower the annual energy consumption by 1–2%;

5) The water consumption of the IEC is in the range of 4–12 L/h. In humid cities, such water consumption can be replenished by the condensate collected from the MVC evaporator, thus eliminating the need for an external water supply.

6) The hybrid system can reduce the annual cost by 15–35%, and the savings are more significant in arid cities.

Data availability statement

The raw data supporting the conclusion of this article will be made available by the authors, without undue reservation.

Author contributions

The contributions of the authors are summarized as follows: QC: Conceptualization, Methodology, Formal analysis, Writing—Original Draft; KM: Methodology, Software, Validation, Investigation; MB: Validation, Formal analysis; MS: Formal analysis; DY: Formal analysis; SO: Formal analysis; XC: Formal analysis; KN: Writing—Review Editing, Supervision, Project administration, Funding acquisition.

Funding

International Graduate School, Tsinghua University (07010100018).

Conflict of interest

The authors declare that the research was conducted in the absence of any commercial or financial relationships that could be construed as a potential conflict of interest.

Publisher's note

All claims expressed in this article are solely those of the authors and do not necessarily represent those of their affiliated organizations, or those of the publisher, the editors and the reviewers. Any product that may be evaluated in this article, or claim that may be made by its manufacturer, is not guaranteed or endorsed by the publisher.

References

Ali, M., Ahmad, W., Sheikh, N. A., Ali, H., Kousar, R., and Rashid, T. u. (2021). Performance enhancement of a cross flow dew point indirect evaporative cooler with circular finned channel geometry. *J. Build. Eng.* 35, 101980. doi:10.1016/j.jobe.2020.101980

Anisimov, S., Pandelidis, D., and Danielewicz, J. (2014). Numerical analysis of selected evaporative exchangers with the Maisotsenko cycle. *Energy Convers. Manag.* 88, 426–441. doi:10.1016/j.enconman.2014.08.055

ANSI/ASHRAE Standard 55-2020 (2020). Thermal environmental conditions for human occupancy. Available at: https://www.ashrae.org/technical-resources/bookstore/standard-55-thermal-environmental-conditions-for-human-occupancy.

Boukhanouf, R., Alharbi, A., Ibrahim, H. G., Amer, O., and Worall, M. (2017). Computer modelling and experimental investigation of building integrated sub-wet bulb temperature evaporative cooling system. *Appl. Therm. Eng.* 115, 201–211. doi:10.1016/j.applthermaleng.2016.12.119

Boukhanouf, R., Amer, O., Ibrahim, H., and Calautit, J. (2018). Design and performance analysis of a regenerative evaporative cooler for cooling of buildings in arid climates. *Build. Environ.* 142, 1–10. doi:10.1016/j.buildenv.2018.06.004

Chen, Q., Burhan, M., Shahzad, M. W., Ybyraiymkul, D., Akhtar, F. H., and Ng, K. C. (2020). Simultaneous production of cooling and freshwater by an integrated indirect evaporative cooling and humidification-dehumidification desalination cycle. *Energy Convers. Manag.* 221, 113169. doi:10.1016/j.enconman.2020.113169

Chen, Q., Ja, M. K., Burhan, M., Shahzad, M. W., Ybyraiymkul, D., Zheng, H., et al. (2022). Experimental study of a sustainable cooling process hybridizing indirect evaporative cooling and mechanical vapor compression. *Energy Rep.* 8, 7945–7956. doi:10.1016/j.egyr.2022.06.019

Chen, Q., Kum Ja, M., Burhan, M., Akhtar, F. H., Shahzad, M. W., Ybyraiymkul, D., et al. (2021). A hybrid indirect evaporative cooling-mechanical vapor compression process for energy-efficient air conditioning. *Energy Convers. Manag.* 248, 114798. doi:10.1016/j.enconman.2021.114798

Cui, X., Chua, K., Islam, M., and Ng, K. (2015). Performance evaluation of an indirect pre-cooling evaporative heat exchanger operating in hot and humid climate. *Energy Convers. Manag.* 102, 140–150. doi:10.1016/j.enconman.2015.02.025

Cui, X., Chua, K., Islam, M., and Yang, W. (2014). Fundamental formulation of a modified LMTD method to study indirect evaporative heat exchangers. *Energy Convers. Manag.* 88, 372–381. doi:10.1016/j.enconman.2014.08.056

Cui, X., Islam, M., and Chua, K. (2019). An experimental and analytical study of a hybrid air-conditioning system in buildings residing in tropics. *Energy Build.* 201, 216–226. doi:10.1016/j.enbuild.2019.06.028

Cui, X., Islam, M., Mohan, B., and Chua, K. (2016). Developing a performance correlation for counter-flow regenerative indirect evaporative heat exchangers with experimental validation. *Appl. Therm. Eng.* 108, 774–784. doi:10.1016/j.applthermaleng.2016.07.189

Cui, X., Sun, L., Zhang, S., and Jin, L. (2019). On the study of a hybrid indirect evaporative pre-cooling system for various climates. *Energies* 12 (23), 4419. doi:10.3390/en12234419

Delfani, S., Esmaeelian, J., Pasdarshahri, H., and Karami, M. (2010). Energy saving potential of an indirect evaporative cooler as a pre-cooling unit for mechanical cooling systems in Iran. *Energy Build.* 42 (11), 2169–2176. doi:10.1016/j.enbuild.2010.07.009

Dizaji, H. S., Hu, E. J., Chen, L., and Pourhedayat, S. (2020). Analytical/experimental sensitivity study of key design and operational parameters of perforated Maisotsenko cooler based on novel wet-surface theory. *Appl. Energy* 262, 114557. doi:10.1016/j.apenergy.2020.114557

Duan, Z., Zhan, C., Zhang, X., Mustafa, M., Zhao, X., Alimohammadisagvand, B., et al. (2012). Indirect evaporative cooling: Past, present and future potentials. *Renew. Sustain. Energy Rev.* 16 (9), 6823–6850. doi:10.1016/j.rser.2012.07.007

Duan, Z., Zhao, X., Liu, J., and Zhang, Q. (2019). Dynamic simulation of a hybrid dew point evaporative cooler and vapour compression refrigerated system for a building using EnergyPlus. *J. Build. Eng.* 21, 287–301. doi:10.1016/j.jobe.2018.10.028

Electricity price in Saudi Arabia (2022). Globalpetrolprices. Available at: https://www.globalpetrolprices.com/Saudi-Arabia/electricity_prices (Accessed on May 20, 2022).

Eveloy, V., and Ayou, D. S. (2019). Sustainable district cooling systems: Status, challenges, and future opportunities, with emphasis on cooling-dominated regions. *Energies* 12 (2), 235. doi:10.3390/en12020235

Heidarinejad, G., and Moshari, S. (2015). Novel modeling of an indirect evaporative cooling system with cross-flow configuration. *Energy Build.* 92, 351–362. doi:10.1016/j.enbuild.2015.01.034

Herrmann, S., Kretzschmar, H.-J., and Gatley, D. P. (2009). Thermodynamic properties of real moist air, dry air, steam, water, and ice (RP-1485). *HVAC&R Res.* 15 (5), 961–986. doi:10.1080/10789669.2009.10390874

Housing GAStat (2018a). Survey data, general authority for statistics, Riyadh, kingdom of Saudi Arabia. Available at: http://www.stats.gov.sa (Accessed May 2nd, 2022).

Housing GAStat (2018b). Survey data, general authority for statistics, Riyadh, kingdom of Saudi Arabia. Available at: http://www.stats.gov.sa (Accessed April 30th, 2022).

Jia, L., Liu, J., Wang, C., Cao, X., and Zhang, Z. (2019). Study of the thermal performance of a novel dew point evaporative cooler. *Appl. Therm. Eng.* 160, 114069. doi:10.1016/j.applthermaleng.2019.114069

Jradi, M., and Riffat, S. (2014). Experimental and numerical investigation of a dew-point cooling system for thermal comfort in buildings. *Appl. Energy* 132, 524–535. doi:10.1016/j.apenergy.2014.07.040

Kabeel, A., and Abdelgaied, M. (2016). Numerical and experimental investigation of a novel configuration of indirect evaporative cooler with internal baffles. *Energy Convers. Manag.* 126, 526–536. doi:10.1016/j.enconman.2016.08.028

Kabeel, A., Bassuoni, M., and Abdelgaied, M. (2017). Experimental study of a novel integrated system of indirect evaporative cooler with internal baffles and evaporative condenser. *Energy Convers. Manag.* 138, 518–525. doi:10.1016/j.enconman.2017.02.025

Krarti, M., Dubey, K., and Howarth, N. (2017). Evaluation of building energy efficiency investment options for the Kingdom of Saudi Arabia. *Energy* 134, 595–610. doi:10.1016/j.energy.2017.05.084

Lee, J., and Lee, D.-Y. (2013). Experimental study of a counter flow regenerative evaporative cooler with finned channels. *Int. J. Heat Mass Transf.* 65, 173–179. doi:10.1016/j.ijheatmasstransfer.2013.05.069

Lopez-Ruiz, H. G., Blazquez, J., and Hasanov, F. (2018). Estimating the Saudi arabian regional GDP using satellite nighttime light images. *SSRN Electron. J.* doi:10.2139/ssrn.3382748

Mikayilov, J. I., Darandary, A., Alyamani, R., Hasanov, F. J., and Alatawi, H. (2020). Regional heterogeneous drivers of electricity demand in Saudi Arabia: Modeling regional residential electricity demand. *Energy Policy* 146, 111796. doi:10.1016/j.enpol.2020.111796

Moshari, S., and Heidarinejad, G. (2017). Analytical estimation of pressure drop in indirect evaporative coolers for power reduction. *Energy Build.* 150, 149–162. doi:10.1016/j.enbuild.2017.05.080

Pandelidis, D., Niemierka, E., Pacak, A., Jadwiszczak, P., Cichon, A., Drag, P., et al. (2020). Performance study of a novel dew point evaporative cooler in the

climate of central Europe using building simulation tools. *Build. Environ.* 181, 107101. doi:10.1016/j.buildenv.2020.107101

Park, J.-Y., Kim, B. J., Yoon, S. Y., Byon, Y. S., and Jeong, J. W. (2019). Experimental analysis of dehumidification performance of an evaporative cooling-assisted internally cooled liquid desiccant dehumidifier. *Appl. Energy* 235, 177–185. doi:10.1016/j.apenergy.2018.10.101

Provinces of Saudi Arabia (2015). Wikipedia subdivisions of Saudi Arabia. Available at: https://en.wikipedia.org/wiki/Subdivisions_of_Saudi_Arabia (Accessed April 25th, 2022).

Rashidi, S., Kashefi, M. H., Kim, K. C., and Samimi-Abianeh, O. (2019). Potentials of porous materials for energy management in heat exchangers–A comprehensive review. *Appl. energy* 243, 206–232. doi:10.1016/j.apenergy.2019.03.200

Riffat, S., and Zhu, J. (2004). Mathematical model of indirect evaporative cooler using porous ceramic and heat pipe. *Appl. Therm. Eng.* 24 (4), 457–470. doi:10.1016/j.applthermaleng.2003.09.011

SAMA (2019). S.A.M.A., ANNUAL STATISTICS 2018. Available at: http://www.sama.gov.sa/en-US/EconomicReports/Pages/YearlyStatistics.aspx (Accessed April 24th, 2022).

Saudi Electricity Company. (2015) *Annual report.* Available at: https://www.se.com.sa/en-us/Pages/AnnualReports.aspx (Accessed April 24th, 2022).

Saudi Arabia interest rate (2022). Tradingeconomics. Available at: https://tradingeconomics.com/saudi-arabia/interest-rate (Accessed on May 20, 2022).

Saudi Arabia water price (2022). Globalproductprices. Available at: https://www.globalproductprices.com/Saudi-Arabia/mineral_water_prices/(Accessed on May 20, 2022).

Shahzad, M. W., Burhan, M., Ybyraiymkul, D., Oh, S. J., and Ng, K. C. (2019). An improved indirect evaporative cooler experimental investigation. *Appl. Energy* 256, 113934. doi:10.1016/j.apenergy.2019.113934

Shahzad, M. W., Lin, J., Xu, B. B., Dala, L., Chen, Q., Burhan, M., et al. (2021). A spatiotemporal indirect evaporative cooler enabled by transiently interceding water mist. *Energy* 217, 119352. doi:10.1016/j.energy.2020.119352

Vargas Bautista, J. P. (2014). Heat recovery system in an industrial furnace to generate air conditioning through an absorption chiller. *I&D.* 1 (14), 117–134. doi:10.23881/idupbo.014.1-7i

Wang, F., Sun, T., Huang, X., Chen, Y., and Yang, H. (2017). Experimental research on a novel porous ceramic tube type indirect evaporative cooler. *Appl. Therm. Eng.* 125, 1191–1199. doi:10.1016/j.applthermaleng.2017.07.111

Wunderground (2022). Wunderground. Available at: https://www.wunderground.com/history/daily/sa/jeddah/OEJN/date/2021-12-10 (Accessed Apr 24th, 2022).

Zanchini, E., and Naldi, C. (2019). Energy saving obtainable by applying a commercially available M-cycle evaporative cooling system to the air conditioning of an office building in North Italy. *Energy* 179, 975–988. doi:10.1016/j.energy.2019.05.065

Zhao, X., Liu, S., and Riffat, S. B. (2008). Comparative study of heat and mass exchanging materials for indirect evaporative cooling systems. *Build. Environ.* 43 (11), 1902–1911. doi:10.1016/j.buildenv.2007.11.009

Zhu, G., Chow, T.-T., and Lee, C. (2017). Performance analysis of counter-flow regenerative heat and mass exchanger for indirect evaporative cooling based on data-driven model. *Energy Build.* 155, 503–512. doi:10.1016/j.enbuild.2017.09.053

Nomenclature

Abbreviations

CDD Cooling degree days, °C-day/year

CDH Cooling degree hours, °C-hr/year

COP Coefficient of performance

DGH Dehumidifying gram hours, g-hr/year

IEC Indirect evaporative cooler

MVC Mechanical vapor compressor

RH Relative humidity, %

Symbols

h Enthalpy, kJ/kg

m Mass flowrate, kg/s

P Power, W

T Temperature, °C

Greek letters

ε Enthalpy effectiveness of IEC, %

φ Contribution of IEC to overall cooling load, %

ω Humidity ratio, g/kg

Subscripts

OA Outdoor air

CA Pre-cooled air from IEC

SA Supply air

RA Return air

WA Wet air

PA Purge air

sat Saturation

pump Water pump

fan Fan

comp Compressor